Time-optimal variational control of a bright matter-wave soliton

Time-optimal variational control of a bright matter-wave soliton

Tang-You Huang [1,2] Jia Zhang [1] Jing Li,[3] and Xi Chen [1,2,*]

[1]*International Center of Quantum Artificial Intelligence for Science and Technology (QuArtist),*
and Department of Physics, Shanghai University, 200444 Shanghai, China
[2]*Department of Physical Chemistry, University of the Basque Country UPV/EHU, Apartado 644, 48080 Bilbao, Spain*
[3]*Quantum Systems Unit, Okinawa Institute of Science and Technology Graduate University, Onna, Okinawa 904-0495, Japan*

Motivated by recent experiments, we present the time-optimal variational control of a bright matter-wave soliton trapped in the harmonic trap by manipulating the atomic interaction through Feshbach resonances. More specifically, we first apply the variational technique to derive the motion equation for capturing the soliton's shape and, second, combine an inverse-engineering method with optimal control theory to design the scatter length for implementing time-optimal decompression. Since the minimum-time solution is of the "bang-bang" type, the smooth regularization is further adopted to smooth the on-off controller out, thus avoiding the heating and atom loss induced from the magnetic field ramp across a Feshbach resonance, in practice.

I. INTRODUCTION

The experimental discovery of Bose-Einstein condensates (BECs) in 1995 has instigated a broad interest in ultracold atoms and molecules [1–3], and paved the way for extensive studies of the nonlinear properties and dynamics of Bose gases, with the applications in atom optics and other areas of condensed-matter physics and fluid dynamics [4]. For atomic matter waves, the matter-wave soliton can be experimentally created in BECs with repulsive and attractive interaction between atoms, which indicates a dark soliton [5,6] and bright soliton [7,8] respectively. Subsequently, more experimental findings show the formation of bright solitary matter waves and probe for potential barriers [9–12]. Very recently, the bright solitons were created by a double-quench protocol, that is, by a quench of the interactions and the longitudinal confinement [13]. In this regard, bright solitons, i.e., a nonspreading localized wave packet, are the most striking paradigm of a nonlinear system since a bright soliton and bright solitary waves are excellent candidates for applications in highly sensitive atom interferometry [14–16] or the generation of the Bell state in quantum information processing [17].

In the mean-field approximation, an atomic BEC obeys the Gross-Pitaevskii (GP) equation, which is equivalent to the three-dimensional (3D) nonlinear Schrödinger equation, while in a quasi-one-dimensional (1D) regime, these systems with BECs confined in a cigar-shaped potential trap are reduced to the 1D GP equation [18]. In particular, with the experimental feasibility of reaching the quasi-1D limit of true solitons, the modulation of the scattering length by varying the magnetic field through a board Feshbach resonance gives rise to prominent nonlinear features, such as collapse [19,20], collision [21], and instability [22]. In most aforementioned

experiments [7–13,20–22], the quenching of atom interactions from repulsive to attractive makes the cloud unstable, resulting in the excitation of breathing modes [13]. Meanwhile, the experimentally observed atom loss rate, relevant to inelastic three-body collisions, becomes orders of magnitude larger than one would expect for a static soliton [23]. Therefore, shortcuts to adiabaticity (STA) [24,25] are requested to surpass the common nonadiabatic process, for instance, thus avoiding the significant heating and losses induced from the sudden switching of the atomic interactions [26].

By now, the variational technique, originally proposed in a nonlinear problem [27,28], has been developed for STA in particular systems [29–32] that cannot be treated by means of other existing approaches, i.e., invariant-based engineering [33,34], counterdiabatic driving [35–37], and fast-forward scaling [38,39]. More specifically, since the time-dependent variational principle can find a set of Newton-like ordinary differential equations for the parameters (i.e., the width of cloud, center, and interatomic interaction), the variational control provides a promising alternative aimed at accelerating the adiabatic compression or decompression of BECs and bright solitons [29,32], beyond the harmonic approximation of the potential [31] and Thomas-Fermi limit [33,40,41]. In this scenario, the Lewis-Riesenfeld dynamical invariant and general scaling transformations [33,34] are not required in the context of inverse engineering.

In this article, we shall address the time-optimal variational control by focusing on a bright matter-wave soliton trapped in the harmonic trap with tunable interactions [42–44]. Here we first hybridize the variational approximate and inverse-engineering methods to design the atomic interaction, and further apply the Pontryagin's maximum principle in optimal control theory [45] for achieving the time-minimal decompression, fulfilling the appropriate boundary conditions. Under the constraint, the time-optimal solution delivers "bang-bang" control, which requires the dramatic changes

*xchen@shu.edu.cn

of scattering strength around a Feshbach resonance. It turns out that such sudden change leads to the heating and atom loss, excites the breathing modes, and thus makes the practical experiment unstable or unfeasible [22,23]. Therefore, this motivates us to try the smooth regularization of bang-bang control at the expense of operation time [46,47]. Our results are of interest to deliver an optimally fast but stable creation or transformation of a soliton [13,22,23]. Different from the previous results [26,29,30], the minimum-time control sets a fundamental bound as the quantum speed limit and also has implications in thermodynamic limits of atomic cooling [30–32].

II. VARIATIONAL METHOD OF SOLITON DYNAMICS

We consider a BEC of N atoms of mass m and attractive s-wave scattering length $a_s < 0$, trapped in a prolate, cylindrically symmetric harmonic trap [18,42–44]. To be consistent, we write the dynamics of a BEC described by the following time-dependent 3D GP equation:

$$\left[i\hbar \frac{\partial}{\partial t} + \frac{\hbar^2}{2m} \nabla^2 - U(r) - g_{3D}(t)|\Psi|^2 \right] \Psi = 0, \quad (1)$$

where $\Psi(r, t)$ is the macroscopic wave function (order parameter) of BEC, $g_{3D}(t) = 4N\pi\hbar^2 a_s(t)/m$ is the interatomic strength, proportional to controllable s-wave scattering length $a_s(t)$, and the harmonic trap modeled by

$$U(r) = \frac{1}{2} m[\omega^2 x^2 + \omega_\perp^2 (y^2 + z^2)], \quad (2)$$

with the static longitudinal and transverse trapping frequencies being ω and $\omega_\perp$. Here the time-dependent $a_s(t)$ can be modulated by the external magnetic field through a Feshbach resonance for our proposal.

For sufficiently tight radial confinement ($\omega \ll \omega_\perp$), it is reasonable to assume a reduction to a quasi-1D GP equation by using the wave function [44],

$$\Psi(r, t) = \psi(x, t) \exp[-(y^2 + z^2)/2\sigma_\perp]/\sqrt{\pi \sigma_\perp^2}, \quad (3)$$

with $\sigma_\perp = \sqrt{\hbar/m\omega_\perp}$ being the transverse width, when the traverse energy $E_\perp = \hbar\omega_\perp$. By substituting Eq. (3) into Eq. (1) and integrating the underlying 3D GP equation in the transverse directions, we obtain

$$\left[i\hbar \frac{\partial}{\partial t} + \frac{\hbar^2}{2m} \frac{\partial^2}{\partial x^2} - E_\perp - \frac{1}{2} m\omega^2 x^2 - g_{1D}(t)|\psi|^2 \right] \psi = 0, \quad (4)$$

with $g_{1D}(t) = g_{3D}(t)/2\pi\sigma_\perp^2$. For convenience, we introduce the dimensionless variables with tildes in physical units: $\tilde{t} = \omega_\perp t, \tilde{\omega} = \omega/\omega_\perp, \tilde{x} = x/\sigma_\perp, \tilde{g}(t) = g(t)/\hbar\omega_\perp\sigma_\perp$, with imposed $g(t) \equiv g_{1D}(t) = 2N\hbar\omega_\perp a_s(t)$, such that the reduced 1D GPE equation for wave function $\psi(x, t)$ along the longitudinal direction reads

$$i\frac{\partial \psi}{\partial t} = -\frac{1}{2} \frac{\partial^2 \psi}{\partial x^2} + \frac{1}{2} \omega^2 x^2 \psi + g(t)|\psi|^2 \psi. \quad (5)$$

Here all variables are dimensionless and we ignore the tilde notation from now on, for simplicity.

Since the 1D nonlinear Schrödinger equation supports the ground state in the form of a bright soliton, we consider the standard sech ansatz, instead of the Gaussian ansatz,

$$\psi(x, t) = A(t) \text{sech}\left[\frac{x}{a(t)}\right] e^{ib(t)x^2}, \quad (6)$$

for describing the dynamics, where the amplitude $A(t) = \sqrt{N/2a(t)}$ is normalized by $\int_{-\infty}^{+\infty} |\psi|^2 dx = 2a(t)A^2(t) = N$, $a(t)$ is the longitudinal size of the atomic size, and $b(t)$ represents the chirp and has relevance to currents. In order to apply the time-dependent variational principle [27,28], we write the Lagrangian density $\mathcal{L}$,

$$\mathcal{L} = \frac{i}{2} \left(\frac{\partial \psi}{\partial t} \psi^* - \frac{\partial \psi^*}{\partial t} \psi \right) - \frac{1}{2} |\frac{\partial \psi}{\partial x}|^2 - \frac{1}{2} g(t)|\psi|^4 - \frac{1}{2} \omega x^2 |\psi|^2, \quad (7)$$

where the asterisk denotes complex conjugation. Inserting Eq. (6) into Eq. (7), we calculate a grand Lagrangian by integrating the Lagrangian density over the whole coordinate space, $L = \int_{-\infty}^{+\infty} \mathcal{L} dx$. Applying the Euler-Lagrange formulas $\delta L/\delta p = 0$, where p presents one of the parameters $a(t)$ and $b(t)$, we obtain $b = \dot{a}/2a(t)$ and the following differential equations:

$$\ddot{a} + \omega^2 a(t) = \frac{4}{\pi^2 a^3(t)} + \frac{2g(t)}{\pi^2 a^2(t)}. \quad (8)$$

This resembles the generalized Ermakov equation [32,34], which can be exploited to design STA based on the inverse engineering with the appropriate boundary conditions. The main difference from previous results is that we concentrate on the time modulation of the atomic interaction, instead of trap frequency. In what follows, we shall be concerned with the design STA by quenching the atomic interaction, within minimal time.

III. SHORTCUTS TO ADIABATICITY

The generalized Ermakov equation (8) is analogous to Newton's second differential equation for a fictitious particle with unit mass, with effective potential,

$$U(a) = \frac{1}{2} \omega^2 a^2 + \frac{2}{\pi^2 a^2} + \frac{2g(t)}{\pi^2 a}, \quad (9)$$

as found in Landau's mechanics [48]. In general, the dynamic equation for the width $a(t)$ provides the analytical treatment of the collective mode when ramping the atom-atom interaction suddenly, $g(t) \to 0$ [23]. Here we aim to apply inverse engineering to design the interaction for realizing the speed up of adiabatic expansion when the experimental resolution is improved by creating a bright soliton with a larger longitudinal width [7,44]. Of course, the result can be directly extended to soliton compression [29,49] without any effort.

Along this vein, we consider the fast transformation from the initial state at $t = 0$ to the target one at $t = \tau$, keeping the shape invariant, where the initial width $a(0) = a_i$ ends up with the targets $a(\tau) = a_f$ by adjusting the interaction from $g(0) = g_i$ to $g(\tau) = g_f$. Here, $a_f > a_i$ ($a_f < a_i$) implies the

decompression (compression). To this end, we first introduce the the boundary conditions,

$$a(0) = a_i, a(\tau) = a_f, \tag{10}$$

$$\dot{a}(0) = \dot{a}(\tau) = 0, \tag{11}$$

$$\ddot{a}(0) = \ddot{a}(\tau) = 0, \tag{12}$$

where a_i and a_f are determined by the following equation:

$$a^4 - \frac{2g(t)}{\pi^2\omega^2}a = \frac{4}{\pi^2\omega^2}, \tag{13}$$

when $g(t)$ is specified by the initial and final values, $g(0) = g_i$ and $g(\tau) = g_f$. Equation (13) is the so-called adiabatic reference, resulting from Eq. (8) when the condition $\partial U/\partial a = 0$, yielding $\ddot{a} = 0$, is considered. This is analogous to the perturbative Kepler problem [48], which actually indicates that the fictitious particle stays adiabatically at the minimum of the effective potential (9). Note that the application of boundary conditions for $\ddot{a}$ (12) suggests the smooth changes of atomic interaction at time edges. However, they are essentially not necessary for designing the shortcut protocols, i.e., a bang-bang control. The only concern is that the initial and final states are not the stationary states of the corresponding Hamiltonians, with the sole boundary conditions (10). One may have to change the interaction quickly after the state preparation.

With boundary conditions (10)–(12), we apply the inverse engineering based on Eq. (8). In order to exemplify STA, we choose a simple polynomial ansatz,

$$a(t) = a_i - 6(a_i - a_f)s^5 + 15(a_i - a_f)s^4 - 10(a_i - a_f)s^3, \tag{14}$$

with $s = t/\tau$ and τ being the total time, fulfilling all of the boundary conditions. After we interpolate the function of $a(t)$, the interaction $g(t)$ is eventually designed from Eq. (8). The designed interaction $g(t)$ is smooth, and the switching of the scattering length can be easily implemented in the experiments [7,22]. In principle, the total time τ can be arbitrarily short from the viewpoint of mathematics. The polynomial ansatz is simple, but not optimal at all. We are planning to address the time-optimal control problem with the physical constraint on the atomic interaction.

IV. TIME-OPTIMAL CONTROL AND SMOOTH REGULARIZATION

A. "Bang-bang" control

In general, to minimize the cost function

$$J = \int_0^\tau \mathbf{F}[\mathbf{x}(t), u(t)]dt, \tag{15}$$

the control Hamiltonian H_c, for the dynamical system $\dot{\mathbf{x}} = \mathbf{f}[\mathbf{x}(t), u(t)]$, is defined as

$$H_c(\mathbf{p}, \mathbf{x}, u) = p_0\mathbf{F}[\mathbf{x}(t), u(t)] + \mathbf{p}^T \cdot \mathbf{f}[\mathbf{x}(t), u(t)], \tag{16}$$

where the superscript "T" denotes the transpose of a vector, and $p_0 < 0$ can be chosen for convenience since it amounts to multiplying the cost function by a constant. The Pontryagin's maximum principle states that the coordinates of the extremal

vector $\mathbf{x}$ and of the corresponding adjoint state $\mathbf{p}$, formed by nonzero and continuous Lagrange multipliers, fulfill the Hamiltonian equations, $\dot{\mathbf{x}} = \partial H_c/\partial \mathbf{p}$ and $\dot{\mathbf{p}} = -\partial H_c/\partial \mathbf{x}$, to attain the maximum $H_c(\mathbf{p}, \mathbf{x}, u) = c$ (c being constant) at $u = u(t)$, for almost all $0 \leqslant t \leqslant \tau$ [45].

Now, we introduce $x_1(t) = a$, $x_2(t) = \dot{a}$ and rewrite the dynamics of the system from (8) into two first-order differential equations:

$$\dot{x}_1 = x_2, \tag{17}$$

$$\dot{x}_2 = -\omega^2 x_1 + \frac{4}{\pi^2 x_1^3} + \frac{2u(t)}{\pi^2 x_1^2}, \tag{18}$$

where the bounded control function $u(t) = g(t)$. Without loss of generality, we may simple choose $a_i = 1$, $a_f = \gamma$, $g_i < 0$, and $g_i < g_f$, when $\gamma > 1$ is considered for the decompression of a bright soliton with tunable interaction. We formulate the time-optimal problem that drives the state $\mathbf{x}_i(t) = \{x_1(t), x_2(t)\}$ from the initial $\{1, 0\}$ to final $\{\gamma, 0\}$, under the constraint $g_i \leqslant u(t) \leqslant g_f$.

To find the minimal time τ, we define the cost function,

$$J = \int_0^\tau 1 dt \equiv \tau. \tag{19}$$

Note that the Lagrangian (or running cost) $\mathbf{F}[\mathbf{x}(t), u(t)] = 1$ in the time-optimal problem does not depend on $u(t)$, but the cost J depends on the control $u(t)$ through $\mathbf{x}_i(t)$, which is the trajectory that this control generates. This implies that the minimal time τ relies on the constraint of controller $u(t)$ and the corresponding trajectories; see the discussion below. Here the control Hamiltonian $H_c(\mathbf{p}, \mathbf{x}, u)$ (16) is written as

$$H_c(\mathbf{p}, \mathbf{x}, u) = p_0 + p_1 x_2 - p_2\omega^2 x_1 + \frac{4p_2}{\pi^2 x_1^3} + \frac{2p_2 u(t)}{\pi^2 x_1^2}, \tag{20}$$

with Lagrange multipliers being $\mathbf{p}_i(t) = \{p_1(t), p_2(t)\}$. As a consequence, the Hamiltonian equation gives the explicit expression,

$$\dot{p}_1 = p_2\left(\omega^2 + \frac{12}{\pi^2 x_1^4} + \frac{4u(t)}{\pi^2 x_1^3}\right), \tag{21}$$

$$\dot{p}_2 = -p_1. \tag{22}$$

It is clear that the control Hamiltonian $H_c(\mathbf{p}, \mathbf{x}, u)$ is a linear function of the control variable $u(t)$. Therefore, the maximization of $H_c(\mathbf{p}, \mathbf{x}, u)$ is determined by the sign of the term $2p_2 u(t)/\pi^2 x_1^2$, which is only related with p_2, since the width $a(t)$ is always positive, i.e., $x_1 > 0$, and $p_2 \neq 0$. Here, $p_2 = 0$ does not provide the singular control and only happens at specific instant moments (switching times) [50]. Actually, when the Hamiltonian is linear in the control variable, the application of Pontryagin's maximum principle in optimal control leads to pushing the control to its upper or lower bound depending on the sign of the coefficient of u in the control Hamiltonian [45]. Typically, the optimal control switches from one extreme to the other for the minimum-time problems [40,51], which is referred to as a bang-bang solution. Thus, we can obtain $u(t) = g_f$ when $p_2 > 0$ at time $t \in (0, t_1)$, and $u(t) = g_i$ when $p_2 < 0$ at time $t \in (t_1, t_1 + t_2)$, such that the
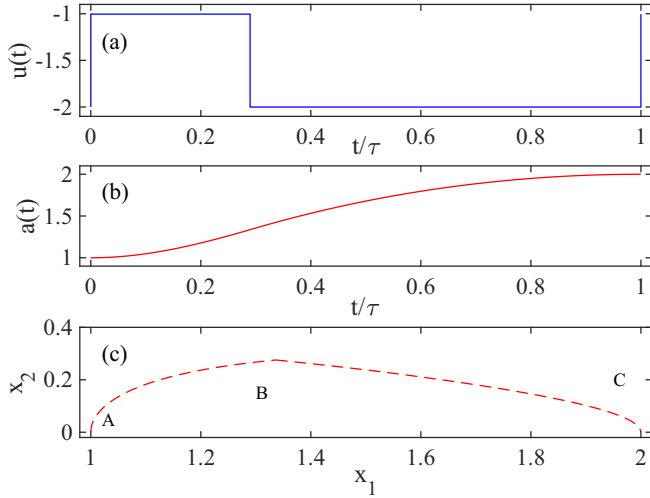
FIG. 1. (a) Controller $u(t)$ of the bang-bang type, for the time-optimal control of soliton decompression. (b) The evolution of $a(t)$, i.e., the width of the bright soliton, is depicted. (c) The trajectory of (x_1, x_2), where the initial point $A = (1, 0)$, intermediate point $B = (x_1^B, x_2^B)$, and final point $C = (\gamma, 0)$ are illustrated. The parameters are $\omega = 0.01$, $\gamma = 2$, $g_i = -2.0005$, $g_f = -1.0039$, and $\tau = 7.0183$ with the switching time $t_1 = 2.0325$.

controller has the form of the bang-bang type [see Fig. 1(a)],

$$u(t) = \begin{cases} g_i, & t = 0 \\ g_f, & 0 < t < t_1 \\ g_i, & t_1 \leqslant t < t_1 + t_2 \\ g_f, & t = t_1 + t_2 = \tau. \end{cases} \quad (23)$$

As a consequence, the time-optimal control suggests the abrupt changes of the controller at the switching times. When control function u is constant, from Eqs. (17) and (18), one can find that x_1 and x_2 satisfy

$$x_2^2 + \omega^2 x_1^2 + \frac{4}{\pi^2 x_1^2} + \frac{4u}{\pi^2 x_1} = c, \quad (24)$$

with constant c. With the bang-bang protocol of controller (23), the system evolves from the initial point $A(1, 0)$, along the intermediate one $B(x_1^B, x_2^B)$, and finally ends up with the target point $C(\gamma, 0)$, in the phase space (x_1, x_2).

Next, we manage to calculate the times for two segments, AB and BC, by substituting $u(t) = g_f$ or $u(t) = g_i$ into dynamical equations (17) and (18), respectively. Thus, we have the equation for the first segment AB for $t \in (0, t_1)$,

$$x_2^2 + \omega^2 x_1^2 + \frac{4}{\pi^2 x_1^2} + \frac{4g_f}{\pi^2 x_1} = c_1, \quad (25)$$

with $c_1 = \omega^2 + 4/\pi^2 + 4g_f/\pi^2$, and the second segment BC for $t \in [t_1, t_1 + t_2)$,

$$x_2^2 + \omega^2 x_1^2 + \frac{4}{\pi^2 x_1^2} + \frac{4g_i}{\pi^2 x_1} = c_2, \quad (26)$$

with $c_2 = \omega^2 \gamma^2 + 4/\pi^2 \gamma^2 + 4g_i/\pi^2 \gamma$. The matching condition for the intermediate point $B(x_1^B, x_2^B)$ yields

$$x_1^B = \frac{8g_f^2 \gamma^2}{(\gamma + 1)[(\gamma - 1)(4 - \omega^2 \pi^2 \gamma^2) + 4g_f \gamma]}, \quad (27)$$
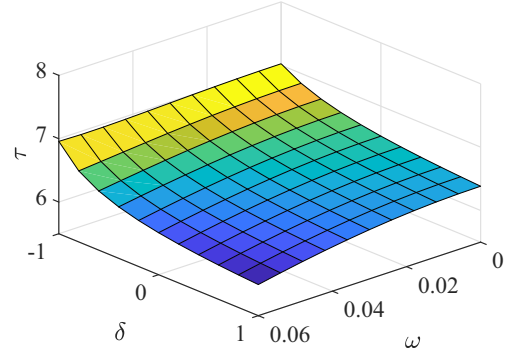

FIG. 2. Minimum time τ vs trap frequency ω and physical constraint δ for bright soliton decompression, where the parameters are the same as those in Fig. 1.

from which we can determine the switching time $t = t_1$ and the total time $\tau = t_1 + t_2$ as follows:

$$\tau = t_1 + t_2, \quad (28)$$

where

$$t_1 = \int_\beta^{x_B} \frac{dx}{\sqrt{c_1 - \omega^2 x^2 - 4/\pi^2 x^2 - 4g_f/\pi^2 x}}, \quad (29)$$

$$t_2 = \int_{x_B}^\gamma \frac{dx}{\sqrt{c_2 - \omega^2 x^2 - 4/\pi^2 x^2 - 4g_i/\pi^2 x}}. \quad (30)$$

Figure 1 illustrate the trajectory of (x_1, x_2), corresponding to the evolution of width a, by using the time-optimal solution of soliton decompression with the controller $u(t)$ of the bang-bang type. Here we take the parameters $\omega = 0.01 \gamma = 2$, $g_i = -2.0005$, and $g_f = -1.0039$. In this case, the minimal time is obtained as $\tau = 7.0183$, with the switching time $t_1 = 2.0325$. Note that the minimal time is different from the cooling process in the time-dependent harmonic trap [32,40,51], where the attractive interaction slows down the cooling process, thus decreasing the cooling rate of the thermodynamic cycle [32].

Furthermore, we display the effect of trap frequency ω and the physical constraint on the minimal time τ in Fig. 2, where the controller $u(t)$ is bounded by $g_i \leqslant u(t) \leqslant \delta$ and other parameters are the same as those in Fig. 1. We visualize that when the same physical constraint is set, the minimal time τ decreases when the trap becomes tight, corresponding to the large trap frequency. Meanwhile, the minimal time τ is decreased, and even approaches zero, when the large constraint δ is allowed. In pursuit of shorter time in the decompression process, the positive region is expected for the constraint δ. Here we emphasize that the minimal time, depending on the trap frequency and atom-atom interaction, has fundamental implications for the efficiency and power in a quantum heat engine with a bright soliton as the working medium [30]. Of course, the STA compression or decompression can replace the adiabatic branches in a quantum refrigerator, clarifying the third law of thermodynamics as well [52].

So far, we attain the minimum-time control of bright-soliton decompression with the bang-bang type; see Eq. (23). This Heaviside function suggests the abrupt changes of interatomic interaction. However, the sudden change of the s-wave scattering length makes the soliton decompression unstable.

When the operation time is much shorter, the interaction changes rapidly from negative and positive by modulating an external magnetic field. This could lead to significant atom loss and heating across a Feshbach resonance.

B. Smooth regularization

Inspired by smooth regularization [47], we reformulate the control function $u(t)$ to $u^\epsilon(t)$ by introducing a real small constant ϵ to avoid the dramatic change in the controller. For this purpose, the system and controller are labeled by the superscript ϵ, yielding the new continuous controller $u^\epsilon(t)$, and the regularized control system $\mathbf{x}_i^\epsilon = (x_1^\epsilon, x_2^\epsilon)$ in the form of

$$u^\epsilon(t) = \frac{(g_i^\epsilon - \delta) p_2^\epsilon}{2\sqrt{[p_2^\epsilon(t)]^2 + \epsilon^2[p_1^\epsilon(t)]^2}}, \tag{31}$$

and

$$\dot{x}_1^\epsilon = x_2^\epsilon, \tag{32}$$

$$\dot{x}_2^\epsilon = -\omega^2 x_1^\epsilon + \frac{4}{\pi^2 (x_1^\epsilon)^3} + \frac{2u^\epsilon(t)}{\pi^2 (x_1^\epsilon)^2}. \tag{33}$$

These guarantee that $u^\epsilon(t)$ reduces to $u(t)$, when $\epsilon = 0$, as seen in the control of the bang-bang type (23). In this scenario, we can have the similar control Hamiltonian $H_c(\mathbf{p}^\epsilon, \mathbf{x}^\epsilon, u^\epsilon)$ as Eq. (20). As a result, the differential equation of the Lagrange multipliers, $\mathbf{p}_i^\epsilon = (p_0^\epsilon, p_1^\epsilon, p_2^\epsilon)$, is obtained as

$$\dot{p}_1^\epsilon = p_2^\epsilon \left(\omega^2 + \frac{12}{\pi^2 (x_1^\epsilon)^4} + \frac{4u^\epsilon(t)}{\pi^2 (x_1^\epsilon)^3} \right), \tag{34}$$

$$\dot{p}_2^\epsilon = -p_1^\epsilon. \tag{35}$$

Here, x_1^ϵ and x_2^ϵ should satisfy the law of energy conservation in Newton's equation [see Eq. (24)], thus yielding

$$(x_2^\epsilon)^2 + \omega^2 (x_1^\epsilon)^2 + \frac{4}{\pi^2 (x_1^\epsilon)^2} + \frac{4u^\epsilon(t)}{\pi^2 x_1^\epsilon} = c^\epsilon. \tag{36}$$

Obviously, the controller $u^\epsilon(t)$ (31) is a continuous function of t, relying on the time-varying p_2^ϵ. Considering the initial and target states, i.e., $[x_1^\epsilon(0), x_2^\epsilon(0)] = (1, 0)$ and $[x_1^\epsilon(\tau^\epsilon), x_2^\epsilon(\tau^\epsilon)] = (\gamma, 0)$, we map the controller $u(t)$ (23) into the following sequence:

$$u^\epsilon(t) = \begin{cases} g_i, & t = 0 \\ \frac{(g_i^\epsilon - \delta) p_2^\epsilon}{2\sqrt{[p_2^\epsilon(t)]^2 + \epsilon^2[p_1^\epsilon(t)]^2}}, & 0 < t < \tau^\epsilon \\ g_f, & t = \tau^\epsilon. \end{cases} \tag{37}$$

By substituting this into Eqs. (32)–(35), we can finally solve the problem with appropriate boundary conditions; see the detailed discussion below.

The central idea of such regulation is the reformulation of bang-bang control by a smooth function in terms of continuous adjoint vector $\mathbf{p}_i(t)$. One can see that by introducing ϵ, we smooth out the control function (31), which drives the interaction $g(t)$ from δ to g_i at switching times, without sudden change [see Fig. 3(a)], where different ϵ are applied for producing the smooth regulation. To understand it better, the corresponding trajectories of $(x_1^\epsilon, x_2^\epsilon)$ and the adjoint vectors $(p_1^\epsilon, p_2^\epsilon)$ are also shown in Figs. 3(b) and 3(c). In the numerical calculation, we use the continuous controller $u^\epsilon(t)$ to solve
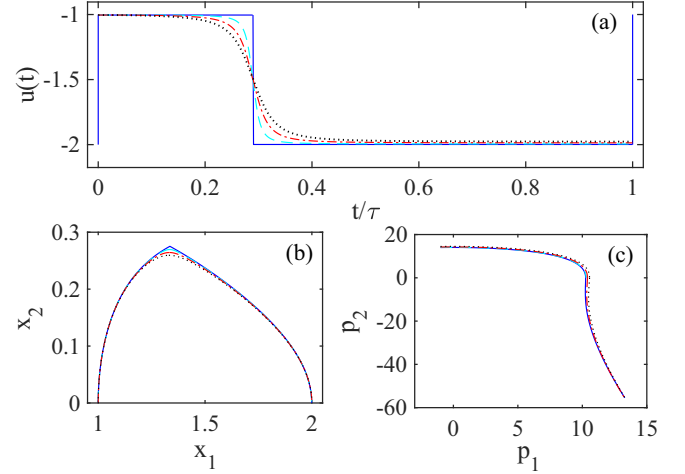

FIG. 3. (a) Smooth controller $u^\epsilon(t)$ with different values: $\epsilon = 0$ (blue solid curve), $\epsilon = 0.1$ (cyan dashed curve), $\epsilon = 0.2$ (red dash-dotted curve), and $\epsilon = 0.3$ (black dotted curve). (b) The trajectory of (x_1, x_2), where the initial point $A = (1, 0)$, intermediate point $B = (x_1^B, x_2^B)$, and final point $C = (\gamma, 0)$ are illustrated, with the related Lagrange multipliers (p_1, p_2) in (c). The fixed δ^ϵ is listed in Table I, and other parameters are the same as those in Fig. 2.

the coupled differential equations [see Eqs. (32)–(35)] for dynamics and adjoint vectors, by using the shooting method. When the controller of the bang-bang type is replaced by the regulated one (31), the total time τ and final state are dependent on the different initial boundary conditions. So we have to introduce two assumptions in the numerical calculation. On one hand, the initial boundary conditions for $p_1^\epsilon(0)$ and $p_2^\epsilon(0)$ should guarantee the maximization of control Hamiltonian $H_c(\mathbf{p}^\epsilon, \mathbf{x}^\epsilon, u^\epsilon)$, i.e., $p_2^\epsilon > 0$ ($p_2^\epsilon < 0$) when $t < t_1$ ($t > t_1$). On the other hand, the constant c^ϵ in Eq. (36) at $t = \tau$, featuring the target state, should be as close as possible to $c(\gamma, 0)$. In detail, we take the $p_1(0) = -1$ and $p_2(0) = 13.9915$ when $\epsilon = 0$ as the reference. Then we simple fix $p_1^\epsilon(0) = -1$ and slightly change $p_2^\epsilon(0)$ to fulfill the aforementioned two conditions. By using the shooting method, we apply the parameters listed in Table I to achieve the suboptimal solution with a smooth controller; see Fig. 3. It turns out that the small deviation g_i^ϵ makes the controller smooth at the cost of operating time τ, with an error of magnitude less than 10^{-3}; see Table I.

V. DISCUSSION

In this section, we will perform the numerical calculation. To this aim, the imaginary-time evolution method is used

TABLE I. The parameters for the shooting method, where we choose $p_1^\epsilon(0) = -1$, and other parameter are the same as in Fig. 3.

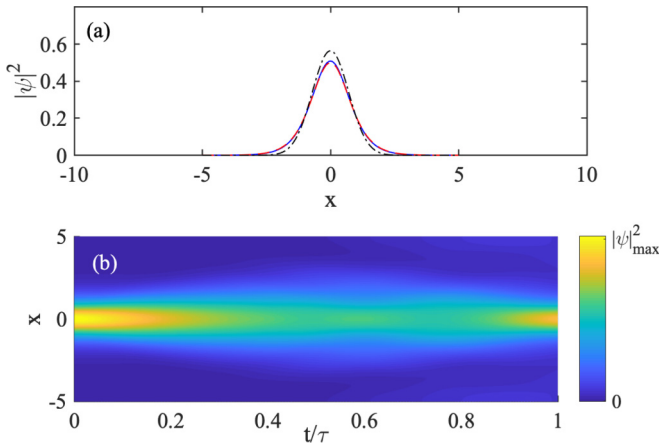| ϵ	g_i^ϵ / g_i	$p_2^\epsilon(0)$	$p_2^\epsilon(t_1)$	$c^\epsilon[\gamma^\epsilon, x_2^\epsilon(\tau)]$
0	1	13.9915	9.9953×10^{-5}	(2,0)
0.1	0.9979	14.1224	7.3087×10^{-5}	(1.9991,0.0013)
0.2	0.9940	14.2316	85770×10^{-5}	(1.9995,0.0031)
0.3	0.9896	14.4910	3.2556×10^{-5}	(1.9998,0.0053)

FIG. 4. (a) Comparison of the sech ansatz (red dashed) and Gaussian (black dot-dashed) ansatz with the initial state (blue solid) calculated from the imaginary-time method, where $g_i = -2.0005$, and trap frequency $\omega = 0.01$. (b) The state evolution $|\psi(x, t)|^2$, numerically calculated from the split operator method, is presented with the parameters in bang-bang control; see Fig. 1.

FIG. 5. (a) Fidelity vs the parameter ϵ with the protocol designed from smooth regularization. The blue solid and red dashed curves present the results obtained from the 1D and 3D simulation, respectively, where the parameters are the same as those in Fig. 1. (b) Fidelity vs the physical constraint δ, for different ϵ, where $\epsilon = 0$ (blue solid), $\epsilon = 0.1$ (red dashed), and $\epsilon = 0.2$ (black dot-dashed), where other parameters are the same as those in Fig. 1.

for obtaining the initial and final stationary states, and the state that is evolving is numerically calculated by means of the split-step method. The validity of the sech ansatz (6), comparing with the Gaussian counterpart, is first checked out. In Fig. 4(a), we confirm that the sech ansatz is more accurate than the Gaussian one for the problem of soliton compression or decompression, when $\omega \ll 1$. The state evolution $|\psi(x, t)|^2$ is carried out by using our designed protocols, starting from the initial state; see Fig. 4(b). Remarkably, by using the time-optimal bang-bang control, the bright-soliton matter wave can be expanded within minimal time. However, during the state evolution, the shape of the soliton is significantly distorted, resulting from abrupt change of the controller u, i.e., the atomic interaction. So the smooth regularization meets the requirement for remedying the difficulties in practical experiments, for instance, the fast adjustment of the magnetic field, or the induced heating or atom loss following magnetic field ramps across a Feshbach resonance.

To quantify the stability, we define the fidelity as $F = |\langle \psi'_f(x)|\psi(x, t_f)\rangle|^2$, where wave function $\psi'_f(x)$ is the final stationary state given by the imaginary-time evolution as well. Figure 5(a) shows that the smooth regulation improves the stability of bang-bang control by smoothing out the controller with the parameter ϵ. Moreover, for larger constraints of δ, the sudden change of atom-atom interaction from negative and positive will make the state evolution unstable. However, the smooth regulation enhances the performance by avoiding the sudden change [see Fig. 5(b)], as compared to the case of bang-bang control. In other words, one can always shorten the operation time by increasing the constraint δ. But it requires the dramatic change of atom-atom interaction by applying an external magnetic field. So, these results demonstrate that there is a trade-off between stability and time, and smooth regulation somehow helps the balance.

In a realistic BEC experiment, such as quench interaction for creating a bright soliton [7] and studying the excitation mode [13], we offer an alternative approach for
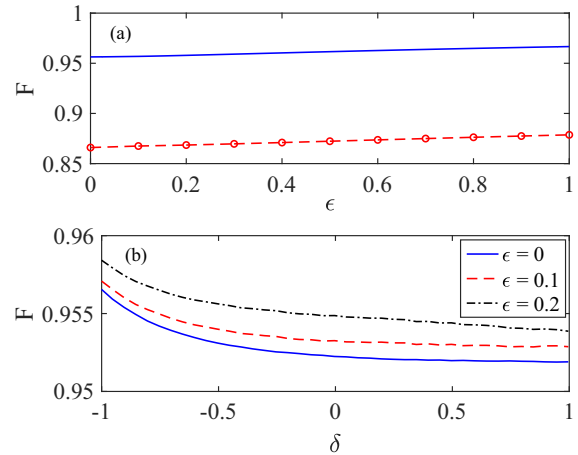
improving unstable experimental conditions. The advantages of smooth bang-bang protocols are twofold. One one hand, the minimum-time protocol makes the soliton expansion as fast as possible to prevent the atom loss, e.g., from inelastic three-body collisions [23]. On the other hand, the smooth controller is easy to implement practically, and can suppress the heating and atom loss induced from the ramp of the interaction. In order to give a reference, we calculate the adiabatic time $\tau^{ad} = 8.25$ ($F > 0.95$) by using the linear ramp, $g(t) = g_i + (g_f - g_i)t/\tau$. When increasing $\gamma = 5$, the minimal time $\tau = 22.4$ becomes much less than the adiabatic one $\tau^{ad} = 179$, showing the advantage of bang-bang control. However, in the quenching process with large γ, the smooth regularization is necessarily required to improve stability by avoiding the dramatic change of controller, i.e., the atomic interaction. In the BEC experiment with ^{7}Li atoms, one can choose the following physical parameters: $\omega_\perp = 710 \times 2\pi$ Hz, $m = 1.1654 \times 10^{-28}$ kg, $N = 2 \times 10^4$, and $\gamma = 2$. Then, our results imply that the minimum-time control of soliton expansion can be experimentally implemented by changing the scattering length, ranging from $a_s(0) = -0.1786$ to $a_s(\tau) = -0.0893$ nm (Bohr radius $a_0 = 5.3$ nm) within the short time 1.5740 ms, which is less than the typical coherent time and adiabatic time $\sim$50 ms for tuning the interaction through slow changes in the magnetic field [7]. Finally, we emphasize that our model is restricted to an effectively 1D trap with a strong transverse confinement. But one may consider the influence of transverse confinement within the framework of 3D GP equation [44] [see Fig. 5(a)], where the dimensionless $g_{3D}(t) = 2\pi g(t)$ in Eq. (1) is used in the numerical calculation, with our designed protocols.

VI. CONCLUSION

In summary, we have studied the variation control of a bright matter-wave soliton in the harmonic trap by

manipulating the atomic interaction through Feshbach resonances. By using the variational approximation, the motion equation is derived for capturing the soliton's shape, without using the Lewis-Riesenfeld dynamical invariant [34] or Thomas-Fermi limit [33,40,41]. Sharing with the concept of STA, we inversely engineer the scatter length, i.e., atom-atom interaction, for achieving the optimally fast but stable soliton decompression. We apply the Pontryagin's maximum principle in optimal control theory to obtain the minimum-time problem, which yields the discontinuous bang-bang protocol. Furthermore, the smooth regularization is further used to smooth out the controller in terms of the shooting method. Though we consider quasi-1D soliton expansion as an example, our results presented here can be easily extended to soliton decompression or compression [29,49], by varying either the trap frequency or the interaction strength or both [13,32], and other nonlinear optical systems [53], by connecting to other methods of enhanced STA working for previously intractable Hamiltonians as well [54]. We find that the experimental relevance can benefit from our smooth time-optimal STA protocols by suppressing the heating and atom losses.

[1] M. H. Anderson, J. R. Ensher, M. R. Matthews, C. E. Wieman, and E. A. Cornell, Science **269**, 198 (1995).

[2] C. C. Bradley, C. A. Sackett, J. J. Tollett, and R. G. Hulet, Phys. Rev. Lett. **75**, 1687 (1995).

[3] K. B. Davis, M. O. Mewes, M. R. Andrews, N. J. van Druten, D. S. Durfee, D. M. Kurn, and W. Ketterle, Phys. Rev. Lett. **75**, 3969 (1995).

[4] F. Dalfovo, S. Giorgini, L. P. Pitaevskii, and S. Stringari, Rev. Mod. Phys. **71**, 463 (1999).

[5] Z. Dutton, M. Budde, C. Slowe, and L. V. Hau, Science **293**, 663 (2001).

[6] S. Burger, K. Bongs, S. Dettmer, W. Ertmer, K. Sengstock, A. Sanpera, G. V. Shlyapnikov, and M. Lewenstein, Phys. Rev. Lett. **83**, 5198 (1999).

[7] L. Khaykovich, F. Schreck, G. Ferrari, T. Bourdel, J. Cubizolles, L. D. Carr, Y. Castin, and C. Salomon, Science **296**, 1290 (2002).

[8] K. E. Strecker, G. B. Partridge, A. G. Truscott, and R. G. Hulet, Nature (London) **417**, 150 (2002).

[9] A. Marchant, T. Billam, T. Wiles, M. Yu, S. Gardiner, and S. Cornish, Nat. Commun. **4**, 1865 (2013).

[10] A. L. Marchant, T. P. Billam, M. M. H. Yu, A. Rakonjac, J. L. Helm, J. Polo, C. Weiss, S. A. Gardiner, and S. L. Cornish, Phys. Rev. A **93**, 021604(R) (2016).

[11] P. J. Everitt, M. A. Sooriyabandara, M. Guasoni, P. B. Wigley, C. H. Wei, G. D. McDonald, K. S. Hardman, P. Manju, J. D. Close, C. C. N. Kuhn, S. S. Szigeti, Y. S. Kivshar, and N. P. Robins, Phys. Rev. A **96**, 041601(R) (2017).

[12] T. Mežnaršič, T. Arh, J. Brence, J. Pišljar, K. Gosar, i. c. v. Gosar, R. Žitko, E. Zupanič, and P. Jeglič, Phys. Rev. A **99**, 033625 (2019).

[13] A. Di Carli, C. D. Colquhoun, G. Henderson, S. Flannigan, G.-L. Oppo, A. J. Daley, S. Kuhr, and E. Haller, Phys. Rev. Lett. **123**, 123602 (2019).

[14] A. Martin and J. Ruostekoski, New J. Phys. **14**, 043040 (2012).

[15] J. L. Helm, S. L. Cornish, and S. A. Gardiner, Phys. Rev. Lett. **114**, 134101 (2015).

[16] G. D. McDonald, C. C. N. Kuhn, K. S. Hardman, S. Bennetts, P. J. Everitt, P. A. Altin, J. E. Debs, J. D. Close, and N. P. Robins, Phys. Rev. Lett. **113**, 013002 (2014).

[17] B. Gertjerenken, T. P. Billam, C. L. Blackley, C. R. Le Sueur, L. Khaykovich, S. L. Cornish, and C. Weiss, Phys. Rev. Lett. **111**, 100406 (2013).

[18] T. P. Billam, S. A. Wrathmall, and S. A. Gardiner, Phys. Rev. A **85**, 013627 (2012).

[19] E. A. Donley, N. R. Claussen, S. L. Cornish, J. L. Roberts, E. A. Cornell, and C. E. Wieman, Nature (London) **412**, 295 (2001).

[20] S. L. Cornish, S. T. Thompson, and C. E. Wieman, Phys. Rev. Lett. **96**, 170401 (2006).

[21] J. H. Nguyen, P. Dyke, D. Luo, B. A. Malomed, and R. G. Hulet, Nat. Phys. **10**, 918 (2014).

[22] J. H. Nguyen, D. Luo, and R. G. Hulet, Science **356**, 422 (2017).

[23] D. Longenecker and E. J. Mueller, Phys. Rev. A **99**, 053618 (2019).

[24] E. Torrontegui, S. Ibáñez, S. Martínez-Garaot, M. Modugno, A. del Campo, D. Guéry-Odelin, A. Ruschhaupt, X. Chen, and J. G. Muga, Adv. At., Mol. Opt. Phys. **62**, 117 (2013).

[25] D. Guéry-Odelin, A. Ruschhaupt, A. Kiely, E. Torrontegui, S. Martínez-Garaot, and J. G. Muga, Rev. Mod. Phys. **91**, 045001 (2019).

[26] M. J. Edmonds, T. P. Billam, S. A. Gardiner, and T. Busch, Phys. Rev. A **98**, 063626 (2018).

[27] V. M. Pérez-García, H. Michinel, J. I. Cirac, M. Lewenstein, and P. Zoller, Phys. Rev. Lett. **77**, 5320 (1996).

[28] V. M. Pérez-García, H. Michinel, J. I. Cirac, M. Lewenstein, and P. Zoller, Phys. Rev. A **56**, 1424 (1997).

[29] J. Li, K. Sun, and X. Chen, Sci. Rep. **6**, 38258 (2016).

[30] J. Li, T. Fogarty, S. Campbell, X. Chen, and Th. Busch, New J. Phys. **20**, 015005 (2018).

[31] T.-N. Xu, J. Li, T. Busch, X. Chen, and T. Fogarty, Phys. Rev. Res. **2**, 023125 (2020).

[32] T.-Y. Huang, B. A. Malomed, and X. Chen, Chaos: Interdiscip. J. Nonlinear Sci. **30**, 053131 (2020).

[33] J. Muga, X. Chen, A. Ruschhaupt, and D. Guéry-Odelin, J. Phys. B: At., Mol. Opt. Phys. **42**, 241001 (2009).

[34] X. Chen, A. Ruschhaupt, S. Schmidt, A. del Campo, D. Guéry-Odelin, and J. G. Muga, Phys. Rev. Lett. **104**, 063002 (2010).

[35] M. V. Berry, J. Phys. A: Math. Theor. **42**, 365303 (2009).

[36] A. del Campo, Phys. Rev. Lett. **111**, 100502 (2013).

[37] S. Deffner, C. Jarzynski, and A. del Campo, Phys. Rev. X **4**, 021013 (2014).

[38] S. Masuda and K. Nakamura, Phys. Rev. A **78**, 062108 (2008).

[39] E. Torrontegui, S. Martínez-Garaot, A. Ruschhaupt, and J. G. Muga, Phys. Rev. A **86**, 013601 (2012).

[40] D. Stefanatos and J.-S. Li, Phys. Rev. A **86**, 063602 (2012).

[41] T. Keller, T. Fogarty, J. Li, and T. Busch, Phys. Rev. Res. **2**, 033335 (2020).

[42] Z. X. Liang, Z. D. Zhang, and W. M. Liu, Phys. Rev. Lett. **94**, 050402 (2005).

[43] L. D. Carr and Y. Castin, Phys. Rev. A **66**, 063602 (2002).

[44] L. Salasnich, Phys. Rev. A **70**, 053617 (2004).

[45] D. E. Kirk, *Optimal Control Theory: An Introduction* (Dover Publications, New York, 2004).

[46] Y. Ding, T.-Y. Huang, K. Paul, M. Hao, and X. Chen, Phys. Rev. A **101**, 063410 (2020).

[47] C. Silva and E. Trélat, IEEE Trans. Autom. Control **55**, 2488 (2010).

[48] L. Landau and E. Lifshitz, *Course of Theoretical Physics. Vol. 1: Mechanics* (Butterworth-Heinemann, Oxford, 1998).

[49] F. K. Abdullaev and M. Salerno, J. Phys. B: At., Mol. Opt. Phys. **36**, 2851 (2003).

[50] X.-J. Lu, X. Chen, J. Alonso, and J. G. Muga, Phys. Rev. A **89**, 023627 (2014).

[51] D. Stefanatos, J. Ruths, and J.-S. Li, Phys. Rev. A **82**, 063422 (2010).

[52] K. Hoffmann, P. Salamon, Y. Rezek, and R. Kosloff, Europhys. Lett. **96**, 60015 (2011).

[53] Q. Kong, H. Ying, and X. Chen, Entropy **22**, 673 (2020).

[54] C. Whitty, A. Kiely, and A. Ruschhaupt, Phys. Rev. Res. **2**, 023360 (2020).